The Red-edge Effect in the Spectra of Fluorenone and 4-Hydroxyfluorenone Alcohol Solutions

M. Józefowicz[a], J. R. Heldt[a], and J. Heldt[a,b]

[a] Institute of Experimental Physics, University of Gdańsk, PL 80-952 Gdańsk, Poland
[b] Institute of Physics, Pomeranian Pedagogical Academy, PL 76-200 Słupsk, Poland

Reprint requests to Dr. J. H.; Fax: (048)(059)341-31-75, E-mail: fizjh@julia.univ.gda.pl

Z. Naturforsch. **57 a,** 787–796 (2002); received May 6, 2002

Photophysical parameters of fluorenone and 4-hydroxyfluorenone have been studied in various solvents using steady state and time-resolved spectroscopic measurements. The fluorescence spectrum of both molecules in hydrogen bonding solvents is inhomogeneously broadened and strongly red shifted in comparison to that determined in nonploar and polar media. At 77 K the fluorescence spectra of the protic solvents are blue shifted (posses a changed intensity distribution) whereas in polar and nonploar one they are red shifted. In H-bond solvents at 77 K the fluorescence spectra of both molecules show an excitation wavelength dependence – *the red-edge effect*. The observed changes of the spectra are confirmed by the results of fluorescence decay measurements. The obtained results are explained by taking into consideration the statistical distribution of the solute-solvent interaction energies and the correlations between the fluorescence rate k_{F}, solvent-cage relaxation rate τ_{R}^{-1} and the vibronic relaxation rate τ_{V}^{-1}.

Key words: Fluorenone; 4-Hydroxyfluorenone; Electronic Spectra; Red-edge Effect.

1. Introduction

Electronically excited molecules in a condensed and liquid phase undergo a rapid ($< 10^{-12}$ s) vibrational relaxation leading to the emitting level of the excited state, which is in thermal equilibrium with the solvent molecules. In some cases, in addition to vibrational relaxation the excited molecular system may undergo other relaxation processes that occur on the nanosecond time scale, e. g. TICT* [1, 2], ESIPT [3, 4], solvent-cage relaxation and initial shock effect [5 - 7], intermolecular excimer formation [8], etc. All the relaxation processes cause distinct changes in the luminescence properties of solute molecules, e. g. the appearance of a new fluorescence band, excitation wavelength dependence of the fluorescence intensity and fluorescence lifetimes, as well as large changes of the Stokes shift and emission anisotropy values observed by changing the excitation wavelength and viscosity of the solvent [1 - 10].

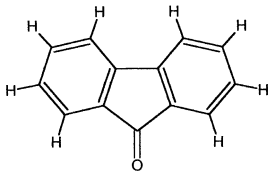

FLUORENONE (9Fl)

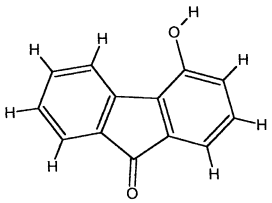

4-HYDROXYFLUORENONE (4HOFl)

Scheme 1. Molecular structure of 9Fl and 4HOFl.

In this paper we present the results of our studies concerning intermolecular proton transfer reactions and solvent-cage relaxation processes appearing in

*Abbreviations. 9Fl - Fluorenone; 4HOFl - 4-Hydroxyfluorenone; H-bond - Hydrogen bonding; TICT - Twisted Intramolecular Charge Transfer; ESIPT - Excited State Intermolecular Proton Transfer; THF - Tertrahydrofuran; EPA - Isopentane-Elhylether-Ethanol; MCH - Methylocyclohexane; H - Hexane; IP - Isopentane; EEP - Diethyl-Ether-Isopentane; EtOH - Ethanol; MeOH - Methanol; CT - Charge Transfer; FWHM - Full Width at Half Maximum.

0932–0784 / 02 / 0900–0787 $ 06.00 © Verlag der Zeitschrift für Naturforschung, Tübingen · www.znaturforsch.com

a fluorescent solution of dipole solute-dipole solvent molecules. The solute molecules are 9Fl and 4HOFl, see Scheme 1. As solvents, spectroscopic grade EtOH, THF, EPA-mixture: isopentane / elhylether / ethanol (5:5:2) were used. The nonpolar solution of MCH and hexane (H) has been used for comparison.

Specific interactions interesting to us mostly occur in inhomogeneous solute-solvents which are controlled by their relaxation towards equilibrium. Depending on temperature of the sample, the reactions are static or dynamic in the sense that the fluorescence decay time τ_F is longer or shorter than averaging of the local states characterized by the vibration time of the Franck-Condon state τ_V and intermolecular proton transfer reaction which is controlled by the solvent-cage relaxation time τ_R. It has been interesting for us to check whether the dissolved 9Fl molecules show a dependence of the fluorescence spectrum on the temperature and rigidity of the polar solvent. The studies of 4-hydroxyfluorenone, have been performed in order to show the differences in the fluorescence emission caused by the proton transfer reaction appearing in the excited state leading to an H-bonded fluorenone complex or by a two-proton relay transfer tautomerisation of 4HOFl. The performed studies indicate that the nearest vicinity of the solute molecule in this two proton-transfer reactions at room temperature and 77 K shows different behaviour during the fluorescence lifetime.

The performed studies comprise steady state and time-resolved spectroscopic measurements of the fluorescence emission of 9Fl and 4HOFl at 293 K and 77 K.

2. Experimental Details

9Fl and 4HOFl were obtained from Aldrich Chemical Co. Before use the compounds were recrystalized from toluene, and their purity was checked chromatographically. The solvents of spectroscopic grade were obtained from E-Merck Ltd. MCH were distilled before use from a sodium potassium amalgam, to ensure their purity and freeness of water.

Absorption spectra measurements were carried out using a Shimadzu UV-2401 PC spectrophotometer. The luminescence emission and the excitation spectra at room temperature and 77 K were recorded on a Shimadzu RF-5301 spectrofluorimeter. The radiation was observed perpendicular to the direction of the exciting beam. For the measurements at room temperature (293 K) rectangular Suprasil 2 and 10 mm cells were used, whereas for those at 77 K suprasil tubes (3 mm in diameter) inserted into liquid nitrogen comprised in the finger of the quartz dewar were applied. The concentration of the solutions studied was ca. $5 \cdot 10^{-4}$ M. The luminescence spectra have been corrected for the spectral response of the photomultiplier (Hamamatsu R-928), but not for reabsorption.

The fluorescence decay curve measurements were performed using the experimental set-up described in [11]. The samples were excited with a spectra-physics picosecond laser system: an argon-pumped Ti-Sapphire-Tsunami 720 - 850 nm laser. The second (360 - 500 nm) or third (240 - 333 nm) harmonic of the Ti-Sapphire laser generates picosecond pulses at a repetition rate in the range from 4 MHz to single shot. The exciting and fluorescence beam were polarised. The fluorescence light is monitored at the magic angle in respect to the polarised exciting beam. The pulse timing and data processing systems employed a biased TAC model TC 864 (Tennelec) and a thermoelectrically cooled emission detector MCP-PMT R3809U-05, equipped with an appropriate Hamamatsu preamplifier. The photon count rate was limited to 20 kHz when the repetition rate of exciting pulses was 4 MHz. The time between the exciting pulses was at least 5-times longer than the measured fluorescence decay time, ensuring excitation of a fully re-equilibrated sample with each laser pulse. The excitation (λ = 320 nm) and emission (at λ_{max} value of the 9Fl and 4HOFl fluorescence spectrum) wavelengths were selected by means of monochromators (about 10 nm bandwidth). The fluorescence decay data were fitted by the interactive convolution to the sum of exponents:

$$I(t) = \sum_i \alpha_i \exp(-t/\tau_i), \tag{1}$$

where α_i and τ_i are the pre-exponential coefficient and the decay time of the i-th fluorescence component, respectively. All time-resolved measurements were performed at room temperature. An exemplary fitting is shown on Fig. 7, where in the panel below the weighted residuals are given. The τ-data collected in Table 1, have a statistical parameter equal to about $\chi^2_R \approx 1$. In the brackets, the participations of the fluorescence intensity components are given.

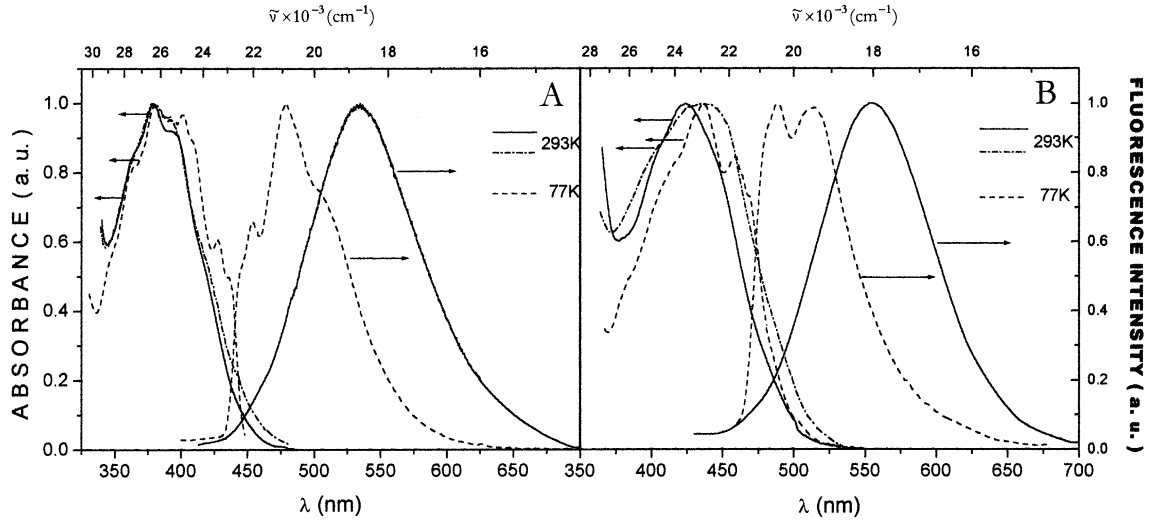

Fig. 1. The longwave absorption (and fluorescence excitation) bands and fluorescence spectra of 9Fl (A) and 4HOFl (B) in EtOH. Concentration of both molecules $c = 5 * 10^{-4}$ M.

3. Results and Discussion

3.1. Steady State Spectroscopic Studies

The solvent and the functional group substitution dependence of the absorption and fluorescence spectra of 9Fl have been the subject of several studies [12 - 19, 32, 33]. It was confirmed that the long wavelength absorption band appears from a state which in polar and nonploar solvents shows a $\pi\pi^*$ or $n\pi^*$ character, respectively. These character changes of the lowest excited singlet state, S_1, have a tremendous influence on the spectroscopic properties of the soluted molecules. In polar protic solvents at room temperature and 77 K an intermolecular hydrogen bonding to the fluorenone oxygen or a proton-relay tautomerization (in the case of 4HOFl) can take place. It induces some additional effects in the solute-solvents surrounding molecules during the lifetime of the excited state S_1 [20].

Figures 1 and 2 show the longwave absorption bands, the fluorescence excitation and the fluorescence emission spectra of 9Fl and 4HOFl dissolved in EtOH and MCH, measured at 77 K and 293 K. The spectra have been also measured for the solvents IP, THF, EPA, and EEP mixtures. Since the spectra of these solutions show similar behaviours as those pictured on Figs. 1 and 2, only some representative spectra are presented. At 77 K the luminescence radiation besides the fluorescence possesses a phosphorescence component with an intensity three orders smaller than that of the fluorescence [13, 19], thus it is neglected in our discussion. The main spectroscopic parameters

Table 1. The λ values at maximum intensity of the longwave absorption band and fluorescence spectrum; its FWHM $\Delta\tilde{\nu}^{A}_{1/2}$ and $\Delta\tilde{\nu}^{F}_{1/2}$ and fluorescence decay times τ_F of 9Fl and 4HOFl in different solutions.

Solvent	λ^A (nm) / $\tilde{\nu}^A\cdot10^3$ (cm^{-1})	λ^F (nm) / $\tilde{\nu}^F\cdot10^3$ (cm^{-1})	$\Delta\tilde{\nu}^{A}_{1/2}$ (cm^{-1})	$\Delta\tilde{\nu}^{F}_{1/2}$ (cm^{-1})	τ_F (ps)
Fluorenone (9Fl):					
Hexane	344.1/26.73	458.3/21.82	4700	3600	131
MCH	374.8/26.68	462.1/21.64	4840	3740	138
			5350**	3260*	
THF	379.6/26.34	479.8/20.84	5110	3670	2730
			6400**	3480*	
EtOH	379.2/26.37	535.2/18.68	5420	3425	41 (4%)
			6430**	3520*	1670 (96%)
4-Hydroxy-fluorenone (4HOFl):					
Hexane	403.2/24.80	471.2/21.22	4710	3500	410
MCH	404.2/24.74	474.6/21.07	5220	3400	430
			4700**	3000*	
THF	418.8/23.88	505.6/19.78	5000	3110	1160
			5930**	2650*	
EtOH	423.8/23.60	550.0/18.18	4830	3090	35 (23%)
			5820**	2870*	270 (63%)
					2560 (14%)

Data without asterisk concern room temperature results.
* $\Delta\tilde{\nu}^{F}_{1/2}$ (77 K), ** $\Delta\tilde{\nu}^{exc}_{1/2}$ (77 K).

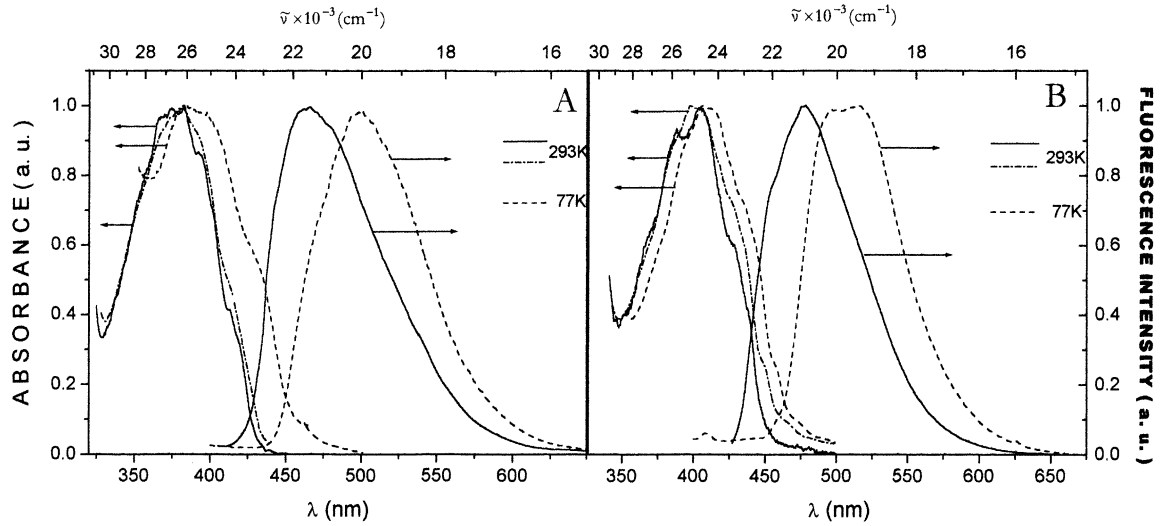

Fig. 2. The longwave absorption (and fluorescence excitation) bands and fluorescence spectra of 9Fl (A) and 4HOFl (B) in MCH. Concentration of both molecules $c = 5 * 10^{-4}$ M.

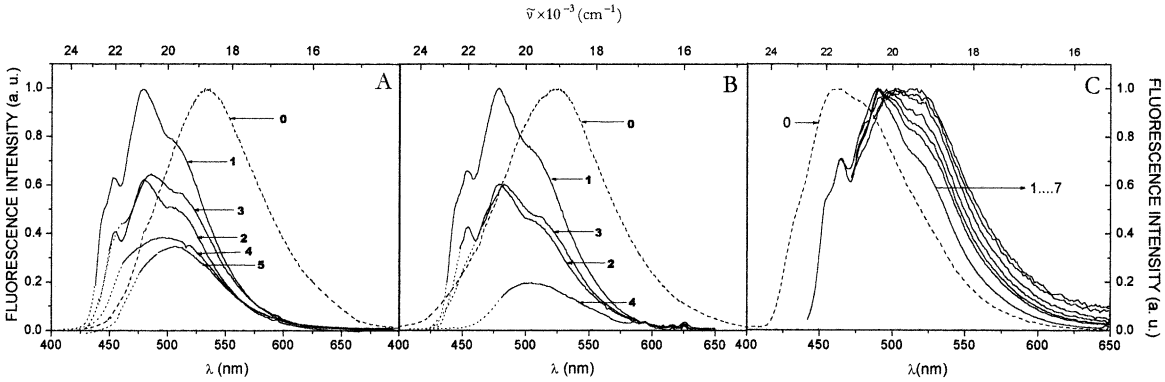

Fig. 3. The excitation wavelength dependence of the fluorescence spectra of 9Fl in EtOH (A), EPA mixture (B) and MCH (C) obtained at 77 K. The curves are obtained for λ_{exc}: 1- 440 nm, 2- 445 nm, 3- 448 nm, 4- 450 nm, 5- 452 nm, 6- 455 nm, 7- 457 nm. The curve denoted by "0" is obtained at 293 K. $c = 5 * 10^{-4}$ M.

of both molecules under study for all solutions used are collected in Table 1.

The absorption spectra (see Figs 1 and 2) of 9Fl and 4HOFl in both solvents possess a very blurred vibrational structure at 293 K. This structure is more distinct in the fluorescence excitation spectra obtained at 77 K. The intensity profile of the fluorescence excitation spectrum of 9Fl at room temperature follows the absorption spectrum well, whereas the spectra obtained at 77 K are batochromic shifted (red-shifted) compared to the $\tilde{\nu}^{A}_{max}$ value of the maximum intensity determined at 293 K. The wave number differences $\tilde{\nu}^{A}_{max} - \tilde{\nu}^{Ex}_{max}$ depend on the solvent and they vary from 1 000 cm^{-1} to 200 cm^{-1}. Generally, for 9Fl the batochromic shift is larger in nonploar solvents than in polar ones. An opposite behaviour is observed for the 4HOFl molecule.

The fluorescence spectrum of both molecules does not show a vibrational structure for all used solutions at room temperature (see Figs. 1 and 2). They are homogeneous, breadent with a symmetric intensity distribution with regard to λ^{F}_{max}. Its λ^{F}_{max} values are 18 800 cm^{-1} for 9Fl and 18 000 cm^{-1} for 4HOFl in the EPA and EtOH solutions. The fluorescence intensity distribution possesses a gaussian shape as expected for a dynamic reaction case [9, 20, 21], i. e.

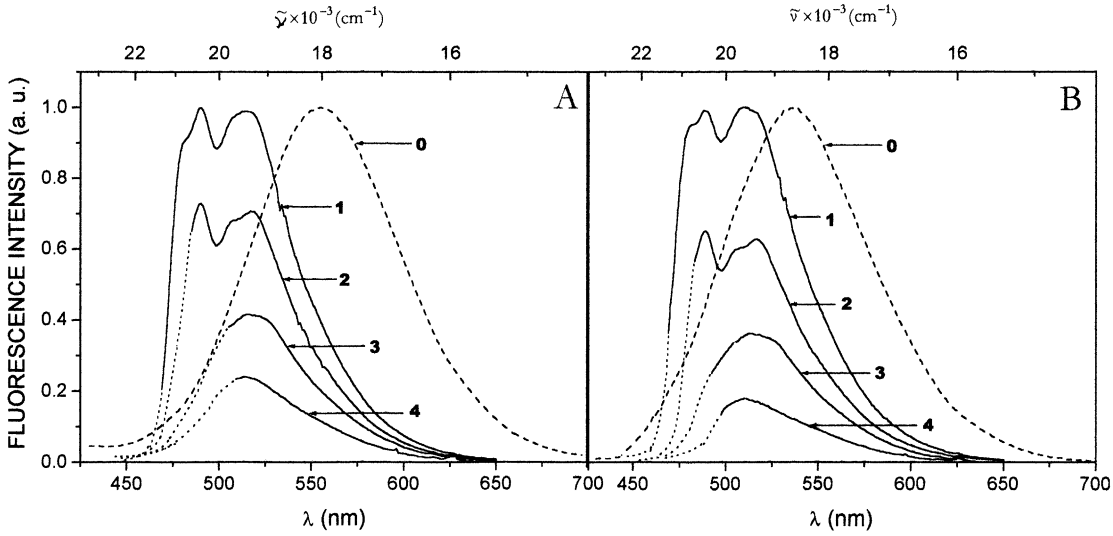

Fig. 4. The excitation wavelength dependence of the fluorescence spectra of 4HOFl in EtOH (A) and EPA mixture (B) obtained at 77 K. The curves are obtained for λ_{exc}: 1- 470 nm, 2- 475 nm, 3- 480 nm, 4- 490 nm. The curve denoted by "0" is obtained at 293 K. $c = 5 * 10^{-4}$ M.

when the motions in the fluorophore environment occur simultaneously or faster than the emission. Its FWHM value $\Delta\tilde{\nu}^{F}_{1/2}$ is smaller than that determined for the long-wave absorption band, $\Delta\tilde{\nu}^{A}_{1/2}$. The differences between $\Delta\tilde{\nu}^{A}_{1/2}$ and $\Delta\tilde{\nu}^{F}_{1/2}$ amounts $\sim 20\,\%$ for nonploar, 30 % polar nonprotic and 37 % for EtOH solvents. The FWHM differences, i. e. $(\Delta\tilde{\nu}^{A}_{1/2} - \Delta\tilde{\nu}^{F}_{1/2})$ are equal (in the error limits of their determination) for the spectra determined at 77 K and 293 K. An exception are the FWHM values determined for the 4HOFl absorption and fluorescence spectra in MCH. In this case the difference of $(\Delta\tilde{\nu}^{A}_{1/2} - \Delta\tilde{\nu}^{F}_{1/2})$ determined for nonploar solutions has the same value as for THF and EtOH solvents. As can be seen on Figs. 1 and 2 and found in Table 1, the $(\Delta\tilde{\nu}^{Ex}_{1/2} - \Delta\tilde{\nu}^{F}_{1/2})$ values differ distinctly from those of $(\Delta\tilde{\nu}^{A}_{1/2} - \Delta\tilde{\nu}^{F}_{1/2})$ determined for MCH, THF and EtOH solutions of both compounds at 77 K. The two values differ by about 25 %. Also the $\tilde{\nu}_{0,0}$ values determined from the spectra obtained at 293 K and 77 K differ. For all solutions the inequality $\tilde{\nu}_{0,0}$ (77 K) > $\tilde{\nu}_{0,0}$ (297 K) is fulfilled.

At 77 K the shape of the fluorescence spectra and the position of its intensity maximum, λ^{F}_{max}, change distinctly; the spectra show a vibrational structure and their intensity maxima are shifted to higher wave numbers (shorter wavelengths) by 2 200 and 2 000 cm^{-1} for 9Fl and 4HOFl, respectively. Noteworthy, the λ-onsets of the fluorescence spectra obtained at 293 K and 77 K are equal (see Figs. 1 and 2).

Fig. 3 and 4 show sets of luminescence spectra of both molecules measured at 77 K, exciting the sample in the Stokes and anti-Stokes region of the absorption spectra. Here, the room temperature fluorescence spectrum is shown for comparison only.

As can be seen on Figs. 3 and 4 the fluorescence spectra of 9Fl and 4HOFl in protic rigid (at 77 K) solvents show an excitation wavelength dependence. It concerns the shape of the fluorescence spectrum and the λ^{F}_{max} value of its intensity maximum. The latter dependence is graphically presented on Figure 5. The dependence of λ^{F}_{max} versus the excitation wavelength is only evident in the anti-Stokes region of the long-wave absorption band. It is more pronounced in the emission spectrum of 9Fl than in 4HOFl (see Figs. 3, 4, and 5). Such an excitation-wavelength dependence is also observed for MCH solutions of 9Fl at concentrations $c > 5 \cdot 10^{-3}$ M (see Fig. 3C). MCH is known as a proton-donating solvent for some molecules [22]. For solutions of lower concentrations and for 4HOFl in MCH and THF at 77 K as well as for all solvents used at room temperature the fluorescence spectrum is independent of λ_{exc} (see Fig. 5).

Our experimental results indicate that the spectra changes induced by varying the temperature as well as the observed fluorescence decay times can be

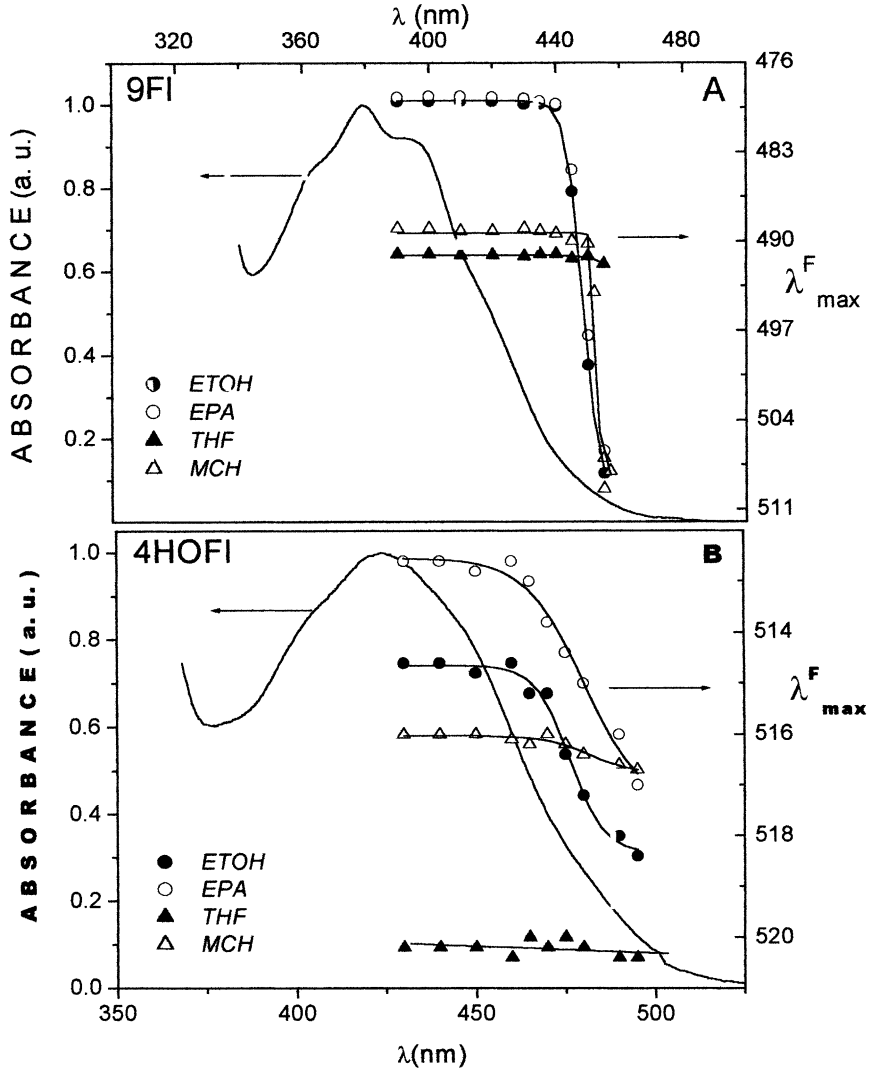

Fig. 5. The excitation wavelength dependence of the fluorescence intensity maximum, λ^{F}_{max}, of 9Fl (A) and 4HOFl (B) determined for various solvents at 77 K. Absorption spectra are given for comparison.

explained assuming that the energy potential curves of the excited and ground state are a two-dimensional double-minimum surfaces as shown on Figure 6.

On Fig. 6 the potential energy cross sections are drawn along two coordinates, Q_v and Q_r, which are the vibrational structure coordinate and the relaxation cage coordinate, respectively. The vibrational coordinate in our case represents a specific vibration which is coupled to the electronic transition whereas the relaxation coordinate, represents the distance between a proton and a specific atom (oxygen) in the molecules studied [9Fl=O...H-OR]. Figure 6 shows a vertical excitation of the molecules from the equilibrium ground state configuration, $S_0^{r,v}$, to a Franck-Condon state, $S_1^{r,v}$, in which both Q_v and Q_r do not change (process 1). As known, the $S_1^{r,v}$ state undergoes a rapid vibrational relaxation (process 2) leading to the S_1^{r,v^0} state, where Q_r does not change but Q_v accedes the vibrational equilibrium excited state configuration, Q_{v^0}. Also, the fluorescence can originate from a $S_1^{r^0,v^0}$ state in which both coordinates aim to take their values in the equilibrium excited configuration (process 7). The creation of a given excited state (i. e. S_1^{r,v^0}, $S_1^{r^0,v^0}$) or an intermediate configuration state (not quantized) depends on the relative magnitudes of the rate constant of the relaxation process, k_R, and the fluorescence decay constant k_F [5, 8, 9, 23].

The vibrational spacing of the absorption and emission spectra at 77 K (see Figs. 1 and 2) is illus-

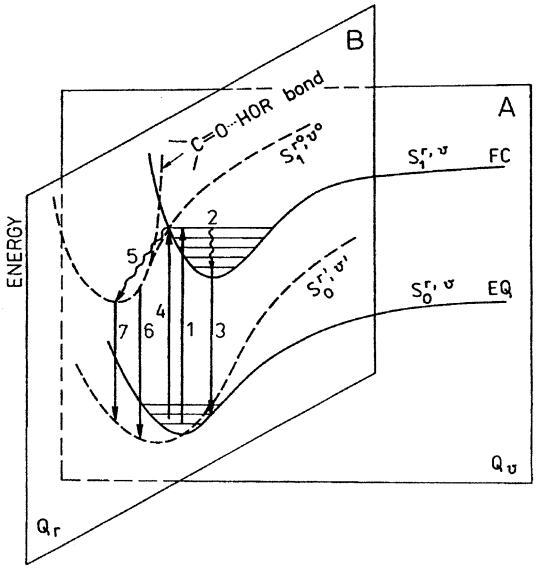

Fig. 6. Schematic representation of the ground and excited state energy surfaces. A and B represent the electronic vibrational energy, Q_V, and the solvent reorganization, Q_r, coordinates respectively. The indicated radiative (1, 3, 4, 6 and 7) and radiationless (2 and 5) transitions are explained in the text.

trated in Fig. 6 (process 1 and 3) by the potential energy cross section along Q_v, which represents the intramolecular vibrational mode coupled to the electronic transition. For the molecules under study the vibrational spacing equals about 900 cm^{-1} in the absorption and fluorescence spectra. The relaxation along Q_r leads to the values of Q_{r^0} of the equilibrium ground and excited state configurations. In the case studied, the energy levels characterizing the potential energy cross-section along Q_r correspond to the frequency modes associated with the not-quantized proton oscillations and solvent shell rearrangements [9Fl=O...H-OR]. In Fig. 6 these processes are indicated by 5 and characterized by the destabilization energy $E_{dest} \cong h\nu^A_{max} - h\nu^F_{max}$ [5].

The Stokes shift values (determined as the difference $\Delta\tilde{\nu}_{St} = \tilde{\nu}^A_{max} - \nu^F_{max}$ or $\tilde{\nu}^{Ex}_{max} - \nu^F_{max}$ at 77 K), correlated to the destabilization energy of the corresponding spectra obtained at room temperature and 77 K, differ significantly (see Table 2). These values depend on the kind of solvent and its temperature. Generally, the Stokes shift at 77 K is smaller than that determined at 293 K. An exception exists for 4HOFl in MCH solution, where an opposite dependence is found. It follows that the E_{dest}-values ob-

Table 2. The maximum intensity wavenumber differences of the longwave absorption and excitation band, $\Delta\tilde{\nu}^A$, of the fluorescence spectra obtained at 293 K and 77 K, $\Delta\tilde{\nu}^F$, the Stokes shift date, $\Delta\tilde{\nu}_{St}$, and destabilization energy, E_{dest}, of 9Fl and 4HOFl in various solutions.

Solvent	$\Delta\tilde{\nu}^A$ $(\tilde{\nu}^A_{293K}-\tilde{\nu}^{exc}_{77K})$ (cm^{-1})	$\Delta\tilde{\nu}^F$ $(\tilde{\nu}^F_{293K}-\tilde{\nu}^F_{77K})$ (cm^{-1})	$\Delta\tilde{\nu}_{St}$ (cm^{-1})	E_{dest} (eV)
Fluorenone (9Fl):				
Hexane			4910	0.59
MCH	890	1280	5040 (4800*)	0.63 (0.59*)
IP	1070	2210	5400 (4840*)	0.67 (0.60*)
THF	600	530	5500 (4080*)	0.68 (0.51*)
EEP	–140	–400	5800 (4350*)	0.72 (0.54*)
EPA	–70	–1700	7200 (4920*)	0.89 (0.61*)
EtOH	0	–2150	7680 (5140*)	0.94 (0.64*)
4-Hydroxy-fluorenone (4HOFl):				
Hexane			3580	0.45
MCH	–130	820	3670 (3710*)	0.46 (0.46*)
THF	1160	–410	4100 (3630*)	0.50 (0.45*)
EEP	400	–600	4200 (3470*)	0.52 (0.43*)
EPA	830	–1930	5250 (3490*)	0.65 (0.43*)
ETOH	630	–1860	5410 (3510*)	0.67 (0.43*)

* Using data determined at 77 K, i. e., $\Delta\tilde{\nu}_{St} = \tilde{\nu}^{exc}_{max}$ (77 K) – $\tilde{\nu}^F_{max}$ (77 K).

tained for nonploar and polar nonprotic solvents are the same within the errors limit and equal to 0.60 eV and 0.46 eV for 9Fl and 4HOFl solutions, respectively. An increase of 50 and 40 percent is found for polar protic solvents (e. g. EtOH, EPA, MeOH etc.) in comparison to values obtained for H, MCH, and THF solutions. Also, the E_{dest} values of 9Fl and 4HOFl determined for the nonprotic and protic solvents at 77 K and 293 K differ by about 15 and 33 percent, respectively. It must be noted that the E_{dest} data of a molecule at 77 K do not depend on the kind of solvent (see Table 2).

The large value of $\Delta\tilde{\nu}_{St}$ points to the existence of strong solute-solvent interactions for the molecules under study [5, 23, 24]. These interactions are exceptionally strong in protic solvents where in the excited state it is very probable that the intermolecular proton-transfer process is responsible for the creation of the respective molecular complexes. For the selected solvents and the molecules under study a considerable blue or red shift of the fluorescence spectra is found on changing the temperature from 293 K to 77 K (see Table 1 and Figs. 1 and 2).

If the equilibrium excited state $S_1^{r^0,v^0}$ is not attained during the lifetime of the excited state, the emission process 6 may occur. The excistence of this process

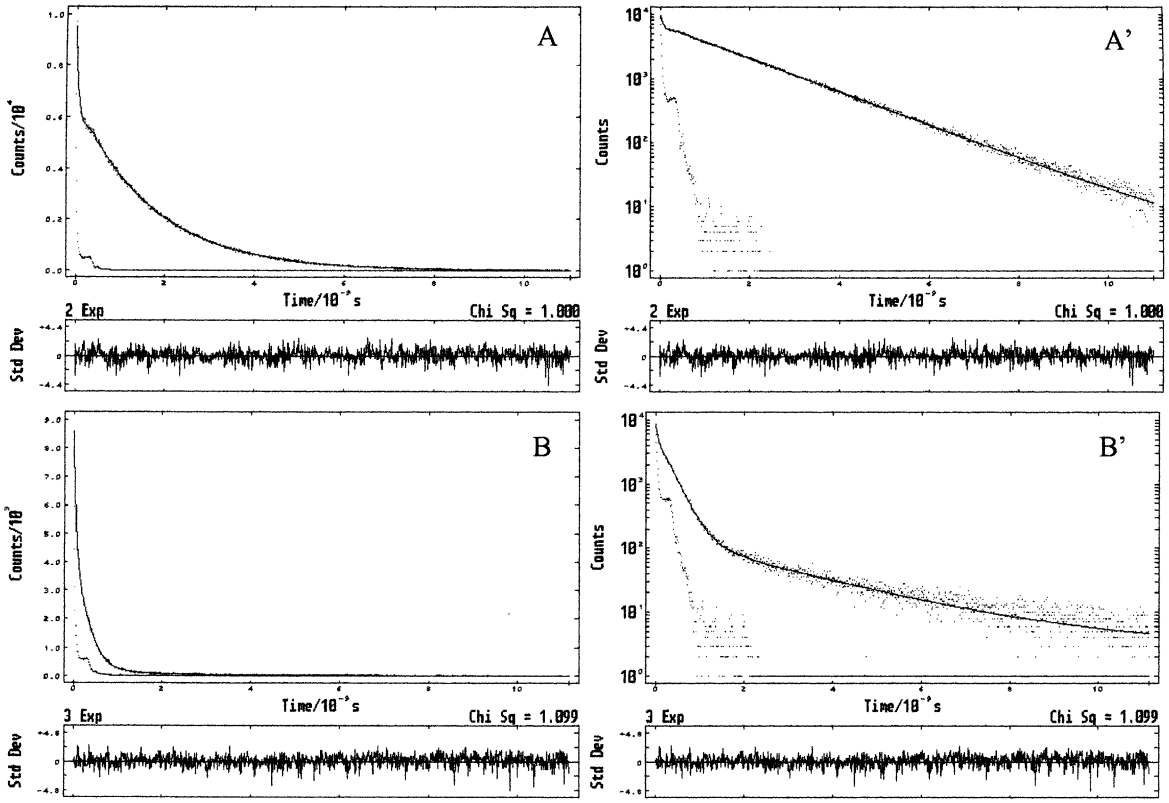

Fig. 7. The fluorescence decay curve of 9Fl (A) and 4HOFl (B) in EtOH solutions at 293 K. In the panels below are given the weighted residuals from fits of these data to sum of exponential. The A' and B' drawings give logaritmic dependence: ln I *versus* t.

explains the excitation-wavelength dependence of the intensity maximum, $\lambda^{\mathrm{F}}_{\mathrm{max}}$, of the fluorescence spectrum (see Figs. 4 and 5).

Ordinary emission (process 3) appears from the thermally equilibrated $S_1^{\pi^0,\nu^0}$ state. The excitation by low-energy quanta ($\leq h\nu_{\mathrm{Reg.}}$) results in photoselection of the low-lying substate of molecules which strongly interact with the solvent molecule, e. g. EtOH. Since there is no quantized coordinate for the solvent structural relaxation of electron transfer [9FL$^-$...EtOH], the emission occurs from the unrelaxed CT state (process 6) with a gaussian shape of the fluorescence spectrum. Emission from the relaxed charge transfer state of the solvent [9FL$^-$...EtOH] is excitation wavelength independent (process 7).

At low temperature there is no solvent reorganization during the fluorescence decay: the emission comes from the same solvent configuration as the excitation. This selective excitation allows to determine the pure emission spectrum of the solvents as well as the activation barrier against solvent reorganization. We can assume that its value (see Figs. 3 and 4) is equal to the difference between $\tilde{\nu}_{00}$ and $\tilde{\nu}^{\mathrm{max}}$ of the associatse i. e. ($\tilde{\nu}_{00}$ (77 K) – $\tilde{\nu}^{\mathrm{max}}_{\mathrm{ass}}$ (77 K). This difference gives following data: 6.43 kcal/M and 4.00 kcal/M for 9Fl and 4HOFl in EtOH, respectively. These values agree well with the data of the hydrogen bond energy [5, 8, 25].

Additionally, the presence of strongly interacting solute-environment cages in the alcohol solutions of both molecules is confirmed by the shift of the fluorescence excitation spectrum to longer wavelength in comparison to the absorption spectrum. The shift mentioned above, determined as ($\tilde{\nu}^{\mathrm{A}}_{\mathrm{max}} - \tilde{\nu}^{\mathrm{Ex}}_{\mathrm{max}}$), equals 300 cm^{-1} for 9Fl and 900 cm^{-1} for 4HOFl. At room temperature the absorption and fluorescence excitation spectra of 9Fl overlap each other, whereas 4HOFl shows a red shift at 293 K and 77 K. Its value is in-

dependent of the observation wavelength of the fluorescence spectrum.

This result is comprehensible if we take into consideration the solvatation shell differences of the two molecules under study and their possible changes during the lifetime of the S_1 state [3, 25, 26]. It is also interesting to record that the mirror symmetry role is well preserved between the fluorescence excitation and fluorescence emission spectra determined at 77 K (see Fig. 1 and 2).

3.2. Time-resolved Emission

In Fig. 7 a typical example of the fluorescence decay data is shown of 9Fl and 4HOFl in EtOH. For this solvent the decay does not follow a simple exponential law (see Figs. 7A' and 7B'). For the other solvent used the fluorescence decay profiles are well described by a mono-exponential fit. The lifetime data obtained using one-exponent and a sum of exponential fitting functions are summarised in Table 1.

The emission decays obtained for 9Fl hexane and MCH solutions agree with the τ data of other authors [15, 21, 27 - 30] and are attributed to the decay from the lowest singlet state with nπ* character. We believe that the decay times 410 ps and 430 ps of 4HOFl in H and MCH characterize the same type of transition.

As is shown in Fig. 7 (see also Table 1), the decay of the fluorescence of both molecules in EtOH can be well fitted by a sum of two or three exponential functions only. These multi-exponential fits can be readily explained using the potential energy scheme given on Figure 6. The emission decays with a lifetime of 40 ps and 35 ps for 9Fl and 4HOFl are well within the instrumental error limit of the emission observed. Nevertheless, we would like to point out that the percentage of its participation in the fluorescence decay depends on the excitation wavelength [13], e. g. is bigger when the sample is excited with $\lambda_{ex} \geq \lambda_{Reg}$. It turns out that the fluorescence compound possessing the short decay time contributes to the total intensity by a rather small amount, i. e. a few percent in the case of 9Fl and about 23 % for 4-hydroxyfluorenone. The contributions of fluorescence decay components are excitation wavelength dependent [13].

Thus we assume that this picoseconed lifetime is associated with a decay from the state of intermediate configuration (unrelaxed CT state, process 6, see Fig. 3) of the hydrogen bonded solvates. The emission decays with lifetimes of 1.67 ns and 2.56 ns for 9Fl and 4HOFl ETOH solutions, respectively, agree with [15, 21, 27 - 30]. They describe the emission from the hydrogen bond and proton-relayd solvates of the molecules under study in the vibrational and relaxation coordinate equilibrium state $S_1^{r^0,v^0}$. The room temperature fluorescence spectrum is broadened. Its shape is described by a gaussian function in agreement with the solvate interation energy distribution noted for not viscous solutions [20, 24, 31]. The λ_{max}^{F} value and the shape of the fluorescence spectra of both molecules under study dissolved in EtOH, MeOH and EPA at room temperature are independent of the excitation wavelength, in agreement with findings made by other authors [9, 20, 21, 23] for molecules showing the red-edge effect.

4. Summary

The steady-state and time-resolved spectroscopic measurements of 9Fl and 4HOFl in protic solvents performed at room temperature and at 77 K point that:

- At 77 K the fluorescence spectra of those molecules in protic solvents show a "blue" frequency shift and a change in shape. The magnitude of the blue frequency shift depends on the solvent.
- The fluorescence excitation spectrum is independent of the fluorescence detection wavelength, λ_{ob}^{F}. The excitation spectrum and the fluorescence spectrum determined at 77 K fulfill the mirror symmetry law.
- We observed the red-edge effect exciting the vitrified samples (at 77 K) of both molecules dissolved in protic solvents. Studying the excitation wavelength dependence of the fluorescence spectrum we determined the emission spectrum of a pure charge-transfer state. This allows to determine the hydrogen bond solute-solvent activation barrier for reorganization of rigid solutions.
- The experimental results show that the destabilization energy and the energy of the active barrier for the reorganization in vitrified protic solvents are different for proton transfer (9Fl) and two-proton relay transfer (4HOFl) reactions of the molecules under study.

The fluorescence quenching phenomena of 9Fl and 4HOFl by different alcoholes will be reported in a future publication [13].

Acknowledgement

This work was partially supported by the research grants of the University of Gdańsk, Project BW-5200-5-0313-2

[1] W. Rettig, Angew. Chem. **98**, 969 (1986).
[2] E. Lippert, W. Rettig, V. Bonacic-Koutecky, F. Heisel, and J. A. Miéhe (1987), Photophysics of Internal Twisting, in Advances in Chemical Physics Ed. I. Prigogine and S. A. Rice, Vol 68.
[3] M. Kasha J. Chem. Soc. Faraday Trans. **82**, 2375 (1986).
[4] W. Klöpffer, Advan. Photochem. **10**, 311 (1977).
[5] N. Mataga and T. Kubota, Molecular Ineractions and Electronic Spectra, Marcel Dekker, New York 1970, Chap. 3 and 7.
[6] A. Jabłoński, Acta Phys. Polon. 26 (1964), 427; Bull. Acad. Polon. Sci., Ser., Sci. Math. Astr. Phys., (1968), **16**, 835.
[7] A. Jabłoński, Bull. Acad. Polon. Sci., Ser., Sci. Math. Astr. Phys. **16**, 835 (1968).
[8] J. B. Birks, Photophysics of Aromatic Molecules, Wiley Interscience, New York 1970, Chap. 7.
[9] A. P. Demchenko, Luminescence and Dynamics of Protein Structure, Naukova Dumka, Kiev 1988, USSR, in Russian.
[10] R. Bauer, H. Grudzinski, E. Lisicki, and A. Jabłoński, Acta Phys. Polon. **33**, 803 (1968).
[11] J. Karolczak, D. Komar, J. Kubicki, M. Szymański, T. Wróżowa, and A. Maciejewski, Bull. Pol. Acad. Sci. Chem. **47**, 361 (1999).
[12] M. Itoh, T. Adachi and K. Tokumura, J. Am. Chem. Soc. **105**, 4828 (1983), and **107**, 4819 (1985).
[13] M. Józefowicz, J. Karolczak, J. R. Heldt, and J. Heldt, Z. Naturforsch., in press.
[14] L. Biczók, T. Bérces, and H. Inoue, J. Phys. Chem. A. **103**, 3837 (1999).
[15] T. Yatsuhashi, Y. Nakajima, T. Shimada, and H. Inoue, J. Phys. Chem. A **102**, 3018 (1998).
[16] R. S. Moog, N. A. Burozski, M. M. Desai, W. R. Good, C. D. Silvers, P. A. Thompson, and J. D. Simon, J. Phys. Chem. **95**, 8466 (1991).
[17] L. J. Andrews, A. Deroulede, and H. Linschitz, J. Chem. Phys. 82, 2304 (1978).
[18] T. Kobayashi and Nagakura, Chem. Phys. Lett. **43**, 429 (1976).
[19] Ch. Huggenberger and H. Labhart, Helvetica Chem. Acta **61**, 250 (1978).
[20] N. A. Nemkovich, A. N. Rubinov, and V. I. Tomin, Inhomogenous Broadening of Electronic Spectra of Dye Molecules in Solutions, Chap. 8 in Topics in Fluorescence Spectroscopy, Ed. J. R. Lakowicz, Plenum Publishing Co., New York 1991.
[21] R. A. Caldwell, Tetrahedron Letters, (1969), **26**, 2121.
[22] A. F. M. Barton, CRC Handbook of solubility parameters and other cohesion parametres, Chap. II, CRC Press, INC. Boca Raton 1985, Florida.
[23] A. P. Demchenko and A. I. Sytnik, Proc. Natl. Acad. Sci. USA, **88**, 9311 (1991).
[24] A. N. Rubinov and V. I. Tomin, J. Appl. Spectrosc. **38**, 42 (1983).
[25] H. Tachikawa, J. Mol. Struct. (Theochem), (1998), 427, 191.
[26] M. Ashraf El-Bayoumi, J. Phys. Chem. **80**, 2259 (1976).
[27] T. Fujii, M. Sano, S. Mishima, and H. Hiratsuka, Bull. Chem. Soc. Japan **69**, 1833 (1996).
[28] R. S. Moog and M. Maroncelli, J. Phys. Chem. **95**, 10359 (1991).
[29] L. Biczok and T. Berces, J. Phys. Chem. **92**, 3842 (1988).
[30] R. S. Murphy, C. P. Moolag, W. H. Green, and C. Bohne, J. Photochem. Photobiol. A. Chem. **110**, 123 (1997).
[31] A. P. Demchenko, J. Luminescence **17**, 19 (2002), and references therein.
[32] J. Herbich, C.-Y. Hung, R. P. Thummel, and J. Waluk, J. Amer. Chem. Soc. **118**, 3508 (1996), and references there in.
[33] A. Kawski and I. Gryczyński, Ber. Bunsenges. Phys. Chem. **80**, 222 (1976).